OPEN ACCESS

CLINICAL SCIENCE

CD19-CAR T-cell therapy induces deep tissue depletion of B cells

Carlo Tur [1,2,3] Markus Eckstein,[4] Joachim Velden,[5] Simon Rauber [1,2]
Christina Bergmann [1,2] Janina Auth,[1,2] Laura Bucci,[1,2] Giulia Corte,[1,2]
Melanie Hagen,[1,2] Andreas Wirsching,[1,2] Ricardo Grieshaber-Bouyer [1,2]
Petra Reis,[1,2] Nicolai Kittan,[1,2] Jochen Wacker,[1,2] Aleix Rius Rigau,[1,2]
Andreas Ramming [1,2] Maria-Antonietta D'Agostino [3] Arndt Hartmann,[4]
Fabian Müller [6] Andreas Mackensen,[6] Aline Bozec [1,2] Georg Schett [1,2,3]
Maria Gabriella Raimondo [1,2]

ABSTRACT

Objectives CD19-targeting chimeric antigen receptor (CAR) T-cell therapy can induce long-term drug-free remission in patients with autoimmune diseases (AIDs). The efficacy of CD19-CAR T-cell therapy is presumably based on deep tissue depletion of B cells; however, such effect has not been proven in humans in vivo.

Methods Sequential ultrasound-guided inguinal lymph node biopsies were performed at baseline and after CD19-CAR T-cell therapy in patients with AIDs. Results were compared with lymph node biopsies from rituximab (RTX)-treated AID patients with absence of peripheral B cells. Conventional and immunohistochemistry staining were performed on lymph node tissue to assess architecture as well the number of B cells, follicular dendritic cells (FDCs), plasma cells, T cells and macrophages.

Results Sequential lymph node biopsies were analysed from five patients with AID before and after CD19-CAR T-cell therapy and from five patients with AID after RTX treatment. In addition, non-lymphoid organ biopsies (colon, kidney and gallbladder) from three additional patients with AID after CD19-CAR T-cell therapy were analysed. CD19+ and CD20+ B cells were completely depleted in the lymph nodes after CD19-CAR T-cell therapy, but not after RTX treatment. Plasma cells, T cells and macrophages in the lymph nodes remained unchanged. Follicular structures were disrupted and FDCs were depleted in the lymph nodes after CD19-CAR T-cell therapy, but not after RTX. Non-lymphoid organs were completely depleted of B cells.

Discussion This study demonstrates complete B-cell depletion in secondary lymphoid tissues of patients with AIDs following CD19-CAR T-cell therapy combined with standard lymphodepleting therapy.

WHAT IS ALREADY KNOWN ON THIS TOPIC
⇒ Treatment with B-cell-targeting chimeric antigen receptor (CAR) T cells has been shown to lead to long-lasting drug-free remission in patients with autoimmune diseases (AIDs). It has been speculated that this effect is based on deep B-cell depletion from the tissues, but no formal proof of this concept has been provided.

WHAT THIS STUDY ADDS
⇒ By performing sequential lymph node biopsies, this study shows that CD19-CAR T-cell administration in conjunction with standard lymphodepleting therapy leads to the complete depletion of B cells from lymph nodes — an effect that has not been observed with antibody-based B-cell depletion therapies, such as the monoclonal anti-CD20 B-cell-targeting antibody rituximab.

HOW THIS STUDY MIGHT AFFECT RESEARCH, PRACTICE OR POLICY
⇒ This study shows a fundamental difference in the depth of cell depletion between antibody-based and cell-based therapeutic approaches. Analysis of secondary lymphoid organs, such as the lymph nodes, can help to gain a better insight into the biological effects of B-cell-targeted therapy in patients with AIDs.

INTRODUCTION
Autoimmune diseases (AIDs) are characterised by the breakdown of immune tolerance, the generation of autoreactive B-cell clones and the production of autoantibodies leading to multi-organ damage. While the clinical manifestations of AIDs, such as systemic lupus erythematosus (SLE), systemic sclerosis (SSc), rheumatoid arthritis (RA) and antineutrophil cytoplasmic antibody-associated vasculitis, are different, they share a common B-cell mediated pathophysiology. B-cell targeting is therefore considered as an important instrument to treat AIDs, which is reflected by the fact that B-cell depleting monoclonal antibodies, such as rituximab (RTX), are widely used in the treatment of AIDs.[1 2] However, RTX only rarely induces drug-free remission in AIDs and some studies even failed to show efficacy of B-cell depletion.[3] While RTX effectively abrogates B cells circulating in the peripheral blood, depletion of B cells in solid tissues and organs is surprisingly much less effective. Thus, synovial tissue, tonsil, bone marrow and lymph node biopsies from RTX-treated patients showed persistence

of B cells in the tissues, suggesting that RTX is unable to achieve deep B-cell depletion.[4–6]

B-cell depletion with CD19-targeting chimeric antigen receptor (CAR) T cells has been recently introduced into the treatment of AIDs.[7–13] Treatment with CD19-CAR T cells has shown to induce long-lasting drug-free remission in patients with SLE and other AIDs, such as idiopathic inflammatory myositis and myasthenia gravis.[9 13] It has been speculated that the long-lasting drug-free remission in the context of CD19-CAR T-cell therapy of AIDs is based on deep depletion of B cells in the tissues and secondary lymphoid organs. However, this concept has so far not been based on data, though CD19-CAR T-cell therapy was able to deplete B cells from the spleen, bone marrow and kidneys in lupus-prone mice.[14] Although it is well documented that CD19-CAR T-cell treated patients with AIDs are depleted of circulating B cells,[7–13] data on tissue B-cell depletion in humans have been lacking to date. Hence, the aim of this study was to investigate B-cell depletion in secondary lymphatic organs of patients with AIDs treated with CD19-CAR T-cell therapy.

PATIENTS AND METHODS
Patients
We analysed inguinal lymph node biopsies from five patients undergoing CD19-CAR T-cell therapy. Biopsies were performed before CD19-CAR T-cell therapy (before the conditioning therapy) and after CD19-CAR T-cell therapy (before the reappearance of B cells) from an inguinal lymph node at baseline and from the homolateral region, following topographic and ultrasound landmarks identified during the previous biopsy, at follow-up. In addition, inguinal lymph node biopsies from five patients treated with RTX were analysed. All five RTX-treated patients had no circulating B cells at the time of the biopsy. Furthermore, non-lymphoid tissue from three additional CD19-CAR T-cell treated patients were assessed.

In particular, tissue from one kidney biopsy (carried out as a diagnostic procedure in the context of proteinuria after CD19-CAR T-cell therapy), one gallbladder specimen (retrieved from cholecystectomy) and one colon biopsy (routine screening colonoscopy) were analysed. When these additional specimens were retrieved, the patients had no circulating B cells.

Lymph node biopsy
The biopsy of inguinal lymph nodes was performed by two rheumatologists (CT/MGR). Briefly, ultrasound evaluation of the inguinal region was performed on patients lying in supine position. Inguinal lymph nodes were identified and long axis diameter was measured. The lymph nodes most easily accessible (according to their distance from vascular and nerve structures) and at a maximum depth of 0.5–1 cm under the skin were chosen. Additionally, only lymph nodes with a long axis diameter greater than at least 0.45 cm were selected. The biopsies were performed under ultrasound-guided approach using a 20 MHz linear probe (Esaote MyLabX90 and Esaote MyLabx80 ultrasound systems). A sterile field was created, and the ultrasound probe was covered by a sterile sheet. Local anaesthesia was obtained using 10 mL of 2% mepivacain and a 0.5 cm skin incision was performed to avoid skin resistance. A 16G semiautomated biopsy core needle (Precisa 1610-HS Hospital Service Spa) was adopted for tissue retrieval. The wound was closed using adhesive plaster. Manual pressure was applied to the biopsied area after each biopsy for at least 2 min and then a sandbag was placed on the biopsy region with the patient resting in supine position for about 30 min to minimise haematoma formation. No further precautions needed to be taken afterwards. The total procedure took 60 min. All biopsies were performed after obtaining individual written informed consent from all patients in accordance with the principles of the Declaration of Helsinki.

Conventional histology and immunohistochemistry
Morphological examination of the tissue specimen was performed by a board-certified pathologist (ME) on H&E-stained tissue sections. Immunohistochemical staining (IHC) was performed using 2 µm thick tissue sections transferred to positively charged adhesive slides (TOMO adhesive slides, Cell-Path, Newton, UK). All staining were performed on a VENTANA BenchMark ULTRA autostainer platform (Ventana, Tucson, USA) according to accredited staining protocols in the routine immunohistochemistry facility of the department of pathology accredited and certified according to DIN EN ISO/IEC 17020. In brief, slides were cut, deparaffinised and further processed on a BenchMark ULTRA autostainer. Antigen retrieval was carried out with CC1 reagent (Ventana) with different incubation times and temperatures (online supplemental table S1A). All lymph node biopsy samples were stained for CD19 (pan B-cell marker), CD20 (pan B-cell marker), CD138 (plasma cells), CD23 (follicular dendritic cells (FDCs)), PD-1 (follicular T helper cells, TFH), Ki67 (MIB1 antigen, proliferation fraction of germinal centre B cells), CD3 (T cells) and CD68 (macrophages). In addition, all lymph node-biopsy samples were assessed with double staining for CD138/CD19 and CD138/Ki67 (online supplemental table S1B).

Stained slides were digitised using a Hamamatsu S210 slide scanner (Hamamatsu) in ×400 magnification and imported into the open source QuPath (V.0.4.3)[15] digital slide analysis environment. The area of interest for cell quantification per mm² tissue area was defined as lymph node parenchyma excluding sclerotic areas and lymph node capsule annotated by a board-certified pathologist (ME). CD3, CD19, CD20, CD68 and CD138 cell populations were automatically quantified, results visually validated and target cell counts per mm² region of interest (ROI) area were reported. To assess the architecture of B-cell maturation compartment (follicular area) of the lymph node a semi-quantitative score integrating general distribution of B cells and B-cell compartment architecture was built. The detailed composition of the score is shown in online supplemental table S2.

Colon, kidney and gallbladder tissue specimens were stained for CD19, CD20, CD3 and CD68 scanned, and annotated by pathologists (ME and JV) as described above. Cells were also automatically quantified per mm² tissue area using QuPath (V.0.4.3).[15]

Double staining for CD138/CD19 and CD138/Ki67 was also assessed using QuPath. In brief, scanned slides were loaded to the QuPath environment and the lymph node region of interest was annotated by a board-certified pathologist (ME). Subsequently, up to 50 single cells per category (categories: CD138⁺ vs CD138⁺Ki67⁺ vs Ki67⁺ or CD138⁺ vs CD138⁺/CD19⁺ vs CD19⁺) were manually annotated as QuPath objects per scanned tissue slide by ME and counterchecked by a second board certified pathologist (AH). These objects were then used to train a single-slide based object classifier using the 'Classify>Train Object Classifier' platform of QuPath relying on the 'Artificial neural network (ANN_MLP)' neural network algorithm to classify all other cell detections based on the trained classifier. Results were then visually validated by ME and AH, and cell populations were quantified per mm² tissue area/area of interest.

Table 1 Patient characteristics

	CD19-CAR-T cells (n=8)	Rituximab (n=5)
Demographic characteristics		
Age, years mean (SD)	33.2 (9.6)	56.8 (7.56)
Sex, female (n)	7	2
Type of autoimmune disease (n)		
SLE	6	0
SSc	2	2
GPA	0	3
Disease duration, months mean (SD)	72.7 (64.96)	44.4 (50.31)
Autoantibodies to (n)		
ANA	8	3
dsDNA	6	0
Scl-70	2	1
Histone	4	1
pANCA	0	1
cANCA	0	3
Others*	5	1
Organ involvement (n)		
Mucocutaneous	8	2
Pulmonary	4	4
Gastrointestinal	1	1
Cardiovascular	2	1
Renal	5	2
MSK	3	0
ENT	0	2
Haematological†	6	0
RTX duration, months mean (SD)	–	20.2 (29.65)
Immunosuppressive medication (n)		
Glucocorticoid	0	1
Other drugs	0	1

Categorical variables: numbers, continuous variables: mean, (SD).
*Each one reactivity in CD19-CAR-T cells: anti-Smith; anti-RNP; anti-SSA/Ro52; anti-SSA/Ro60; anti-SSB; antinucleosome; each one reactivity in RTX: rheumatoid factor.
†Haematological involvement: anaemia 2/6 (1 with evidence of haemolysis), thrombocythemia 1/6, lymphopenia 6/6 according to Easy-BILAG definition.[48]
ANA, antinuclear antibodies; antiSSA/Ro52, anti-Sjögren's syndrome-related antigen A autoantibodies/Ro52; cANCA, antineutrophil cytoplasmic antibodies with diffuse granular, cytoplasmic staining pattern; CAR-T, chimeric antigen receptor T cells; dsDNA, double-stranded DNA; ENT, ear–nose–throat disease; GPA, granulomatosis polyangiitis; MSK, musculoskeletal disease; pANCA, antineutrophil cytoplasmic antibodies with peripheral staining pattern; RNP, ribonucleoprotein; RTX, rituximab; Scl-70, scleroderma 70; SLE, systemic lupus erythematosus; SSA/Ro60, anti-Sjögren's syndrome-related antigen A/Ro60; SSB, anti-Sjogren's syndrome-related antigen B; SSc, systemic sclerosis.

Statistical analysis
Data are presented as medians with IQR or mean ± SD. Differences were analysed with the two-tailed Mann-Whitney U test. The two-tailed Wilcoxon signed-rank test for paired data was used to analyse change after treatment. P values <0.05 were considered statistically significant. All statistical analyses were performed using Prism software (V.10, GraphPad Software, La Jolla, California, USA). An unsupervised hierarchical clustering algorithm (Ward's linkage algorithm, euclidean distance as metric scale) was performed to estimate the B-cell maturation compartment.

RESULTS
Patient characteristics
Details on patient characteristics are summarised in the table 1. In total, eight CD19-CAR T-cell therapy treated patients (six SLE and two SSc) were analysed. In five patients (three SLE and two SSc) sequential inguinal lymph node biopsies were performed before and 60.8 days±5.81 (mean±SD) after CD19-CAR T cells infusion. From the additional three SLE patients treated with CD19-CAR T cells, non-lymphoid tissue was available for analysis. Lymph node biopsies from CD19-CAR T-cell therapy treated patients were additionally compared with lymph node biopsies from five patients with AID (two SSc and three granulomatosis with polyangiitis) that had been treated with RTX (mean (±SD): 98 days (±45.63) after treatment initiation) showing complete absence of peripheral B cells at the time of biopsy (figure 1A). Patients receiving CD19-CAR T-cell therapy displayed longer disease duration (mean (±SD): 72.7 months (±64.96)) as compared with the RTX-treated group (mean (±SD): 44.4 months (±50.31)).

Depletion of peripheral blood B cells and reduction of immunoglobulin (Ig) levels are similar between CD19-CAR T cells and RTX
Circulating B-cell numbers and Ig levels were assessed at the time of lymph node biopsies comparing CD19-CAR T-cell therapy with RTX treatment (figure 1A). Complete depletion of circulating B cells was confirmed in both groups (figure 1A). Circulating CD19-CAR T cells were found at low levels at the time of the second biopsy (mean (±SD): 0.18 cell/µL (±0.24) at day 60), whereas no concomitant peripheral T-cell depletion was observed in the CAR T-cell treated patients (online supplemental figure 1). Both therapies showed a trend towards reduced levels of IgG and IgM, while there was no significant differences between CD19-CAR T-cell treatment (post-treatment IgG levels median (IQR): 829 mg/dL (673.6–1015); post-treatment IgM levels median (IQR): 41.9 mg/dL (15.6–56)) and RTX treatment (IgG levels median (IQR): 997.7 mg/dL (835.9–1274); post-treatment IgM levels median (IQR): 55.4 mg/dL (49.3–78.8)) ($p=0.309$ and $p=0.150$, respectively).

Complete depletion of tissue B cells on CD19-CAR T-cell therapy
Macroscopic dimensions of the inguinal lymph nodes were assessed by ultrasound (figure 1B,C). No statistically significant differences in their size were found before (long axis parameter mean (±SD): 14.7 mm (±2.91)) and after (mean (±SD): 12.7 mm (±7.74); $p=0.750$) CD19-CAR T-cell treatment. Also, the size of the inguinal lymph nodes was similar in the patients that received RTX (mean (±SD): 10.01 (±5.82); $p=0.464$) compared with post-CD19-CAR T-cell treatment. Microscopic evaluation of the B follicle areas in the inguinal lymph node biopsies was assessed by IHC staining of B cells in proximity to FDCs and TFH (online supplemental figure 2). Quantification of B cells was assessed by IHC staining of CD19 and CD20. A complete depletion of CD19$^+$ and CD20$^+$ B cells was observed in the lymph nodes of patients treated with CD19-CAR T cells (pre treatment: CD19$^+$ B cells median (IQR) 656 cells/mm^2 (361–922.5); CD20$^+$ B cells: 1159 cells/mm^2 (549–3771); post treatment: both CD19$^+$ and CD20$^+$ cells=0 cells/mm^2 (0–0)) (figure 1D,E). No such depletion was achieved in the inguinal lymph nodes of patients following RTX treatment, showing persistence of both CD19$^+$ and CD20$^+$ B cells (median (IQR): 196 cells/mm^2 (59.5–1032); 1443 (201.5–2659), respectively) (figure 1D,E).

Some cells expressing the common plasmablast/plasma cell marker CD138$^+$ were still found in the lymph nodes after CD19-CAR T-cell therapy (median (IQR): 166 cells/mm^2
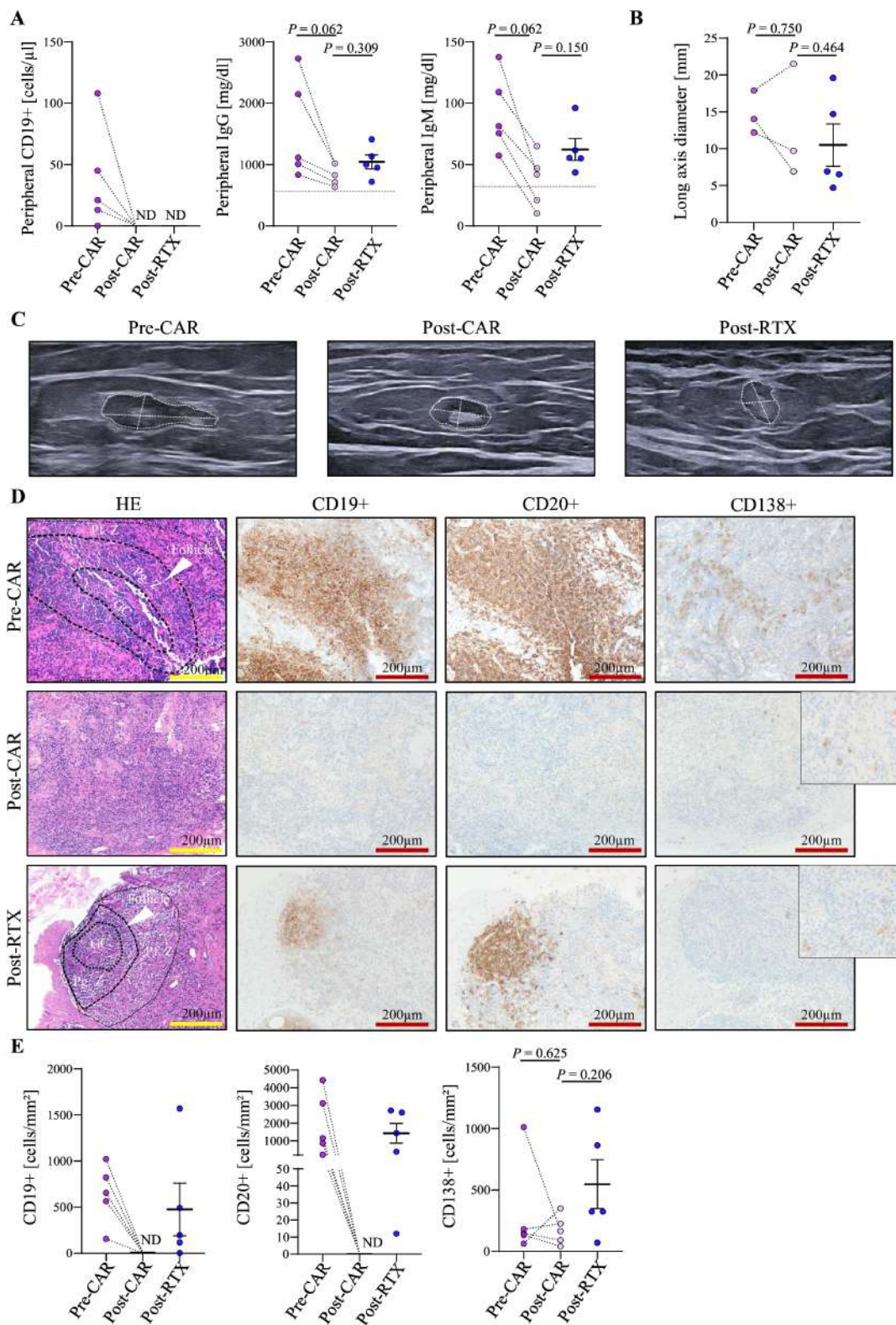
Figure 1 Peripheral blood and lymph node changes on CD19-CAR T-cell treatment. (A) Quantification of CD19$^+$ B cells, IgG and IgM levels in the peripheral blood of patients before (pre-CAR) and after (post-CAR) treatment with CD19-CAR T cells (n=5) and after RTX (post-RTX) treatment (n=5). The dashed horizontal lines indicate lower limit of the normal immunoglobulin range. (B) Quantification of long axis diameter of lymph nodes assessed during biopsy procedure (n=3 pre-CAR and post-CAR; n=5 post-RTX). (C) Representative ultrasound images of inguinal lymph nodes in the same patient before (pre-CAR; left) and after (post-CAR; centre) CD19-CAR T cells and after RTX treatment (post-RTX; right). (D) Representative H&E-stained images of lymph node biopsies obtained from one pre-CAR and post-CAR treated patient and one patient post-RTX, together with representative immunohistochemistry pictures of CD19$^+$ B cells, CD20$^+$ B cells and CD138$^+$ plasma cells. White arrows indicate follicular B-cell areas in the lymph node tissue. (E) Quantification of CD19$^+$ B cells, CD20$^+$ B cells and CD138$^+$ plasma cells in the lymph nodes before (pre-CAR) and after (post-CAR) CD19-CAR T-cell therapy (n=5 patients) and after RTX (post-RTX) (n=5). CAR T, chimeric antigen receptor T cells; GC, germinal centre; ND, non-detectable; Pf. Z, perifollicular zone; Pg. Z, perigerminal zone; RTX, rituximab.

(66–287.5)) and after RTX treatment (median (IQR): 324 cells/mm^2 (197–1010), p = 0.206) (figure 1D,E). In contrast, complete depletion of CD138$^+$ CD19$^+$ plasmablasts was observed after CAR T-cell therapy (pre treatment: median (IQR) 25 cells/mm^2 (11.5–41); post treatment: median (IQR) 0 cells/mm^2 (0–0)), but not after RTX treatment (median (IQR) 2 cells/mm^2 (0.5 – 13)). Notably, plasma cells displayed a lower proliferation rate after CAR T-cell therapy as compared with RTX (post-CAR T-cell therapy: median (IQR) 5 cells/mm^2 (2–10.5); post-RTX: median (IQR) 35 cells/mm^2 (9.5–53.5); p=0.039) (online supplemental figure 3).

B-cell depletion was also confirmed as auxiliary finding in non-lymphoid tissues. In particular, colon, kidney and gallbladder specimens showed no B cells, 86, 30 and 7 days after CAR T-cell infusion, respectively, whereas T cells and macrophages were present (online supplemental figure 4).

Disappearance of follicular structures in the lymph nodes after CD19-CAR T-cell therapy

We next assessed changes in the follicular structure of the lymph node after CD19-CAR T-cell therapy, including FDCs, TFH cells and proliferation rate in the follicles before and after treatment (figure 2A). These measurements were included to build a combined B-cell compartment architecture score (figure 2B,C). In RTX-treated patients, the FDC network and the presence of TFH cells were mostly unaltered, accompanied by regular (>90%) or slightly reduced germinal centre proliferation rates (median B-cell compartment score (IQR): 10 (8.5–14)). In contrast, while regularly configured in pre-CAR T-cell state (median B-cell compartment score (IQR): 14 (14–14)), the B-cell maturation compartment was completely abolished after CD19-CAR T-cell treatment including disappearance of FDC networks and TFH cells as well as decrease (<90%) of proliferation rate (median B-cell compartment score (IQR): 0 (0–0.5)).

These changes described in the B-cell compartment of the lymph node did not affect the distribution of T cells and macrophages, which remained stable after CD19-CAR T-cell therapy (CD68$^+$ pretreatment median (IQR): 3010 cells/mm^2 (2316–3795), post treatment: 2439 cells/mm^2 (2042–2968)); CD3$^+$ pre treatment: 3834 cells/mm^2 (1943–5032)), post treatment: 2847 cells/mm^2 (1751–4377)) (figure 2D,E). Moreover, no difference in macrophages was found between CD19-CAR T-cell therapy and RTX-treated patients (CD68$^+$ median (IQR): 2061 cells/mm^2 (1755–4216); p>0.999). The overall number of T cells was higher in the RTX group than in the pre-CD19-CAR and post-CD19-CAR T-cell treatment groups.

DISCUSSION

This study demonstrates that CD19-CAR T-cell therapy induces deep B-cell depletion in lymphoid tissues. The depletion was complete across all patients, regardless of the disease and was consistent with the depletion observed in the peripheral blood at the time of biopsy. Deep depletion was accompanied by an abrogation of FDCs and follicular structure in the lymph nodes. In addition, no B cells were observed in biopsies of non-lymphoid organs, taken from three additional patients at different intervals post-CD19-CAR T-cell therapy, further confirming the complete B-cell depletion by cell-based therapy.

Ultrasound-guided lymph node biopsy has been previously used in AIDs and has been described as safe, well-tolerated and useful approach for studying the lymph node composition of patients with RA.[16][17] Analysis of tissues retrieved as early as 30 days after RTX treatment has shown that RTX does not necessarily deplete B cells in the lymph nodes despite showing complete depletion in the peripheral blood.[5][6] In agreement with these previous reports, we did not observe a complete depletion of B cells in the lymph nodes after an average of 98 days post-RTX treatment, despite persistence of B-cell depletion in the periphery. Circulating B cells usually reconstitute between 84 and 224 days after exposure to RTX.[18–20] Incomplete depletion of tissue B cells by RTX, despite complete depletion of circulating B cells, is supported by additional studies from the spleen of patients with autoimmune thrombocytopenia and in the synovium and bone marrow from patients with RA.[21–23] In CD19-CAR T-cell treated patients, post-treatment biopsy was performed in the absence of peripheral B cells, which usually recur 65–159 days after CAR T-cell exposure.[9]

A newer generation of B-cell depleting antibodies, such as the anti-CD20 monoclonal antibody, obinutuzumab, may induce deeper tissue B-cell depletion due to better antibody-dependent cellular cytotoxicity. So far, only one report on obinutuzumab showed a good but not complete B-cell depletion in the lymph nodes of kidney transplant patients.[24] Bispecific T-cell engagers, such as blinatumomab, also induce peripheral B-cell depletion.[25] So far, anecdotal evidence suggests good but not complete tissue B-cell depletion in a liver metastasis from a cancer patient[26] and in the synovial tissue of patients with RA.[27] However, no data on the effects of blinatumomab or other T-cell engagers on B-cell depletion in the lymphoid organs are currently available.

B-cell depletion was also observed in three different non-lymphoid organs. Although pretreatment samples of the same tissues were not available for comparative analysis, it is known that resident B cells can colonise these organs in physiological or inflammatory conditions.[28–30] These data further support complete tissue B-cell depletion by CAR T-cell therapy.

We also observed that B-cell depletion by CD19-CAR T cells, but not by RTX, led to the disappearance of germinal centre structures. Hence, effects of CD19-CAR T-cell treatment were not only limited to B cells, but also affected FDCs. Previous data reported the expression of CD19 molecule on FDCs,[31] suggesting a possible eradication of these cells mediated by CD19-CAR T cells. On the other hand, FDCs, which are in fact of mesenchymal origin,[32] may not genuinely express CD19 but may have taken it up from B cells by a process called trogocytosis. In vivo data showed an interdependence between B cells and FDCs.[33] Ontogenetic studies on secondary lymphoid organs in vivo showed that B cells are the first populating the lymphoid tissue before FDCs appear.[34] Indeed, the presence of B cells seems essential for the development of FDCs and has been shown to rely on lymphotoxin-β signalling.[35] As a proof of concept, B-cell depleted mice also showed a depletion of FDCs.[36–38] As the initial population of the lymph nodes in mice was independent of the FDC–CXCL13 axis,[34] repopulation of lymph nodes in patients after CD19-CAR T-cell therapy may also occur in a similar FDC-independent manner. On the same line, B cells are essential for TFH survival via the ICOS-L/ICOS and CD40/CD154 signalling pathways and B-cell depletion in vivo resulted in alteration of TFH.[39][40] So far, no data have shown an impact of RTX on FDCs, which can be explained by the incapacity of RTX to induce complete B-cell depletion in secondary lymphoid organs. On the other hand, a reduction of TFH numbers was observed in the spleen of patients with immune thrombocytopenia treated with RTX.[41]

Our data show that CD19-CD138+ plasma cells were not reduced by CD19-CAR T-cell therapy in the lymph nodes. However, we observed a complete depletion of the CD19$^+$CD138$^+$ plasmablasts after CD19-CAR T-cell treatment.
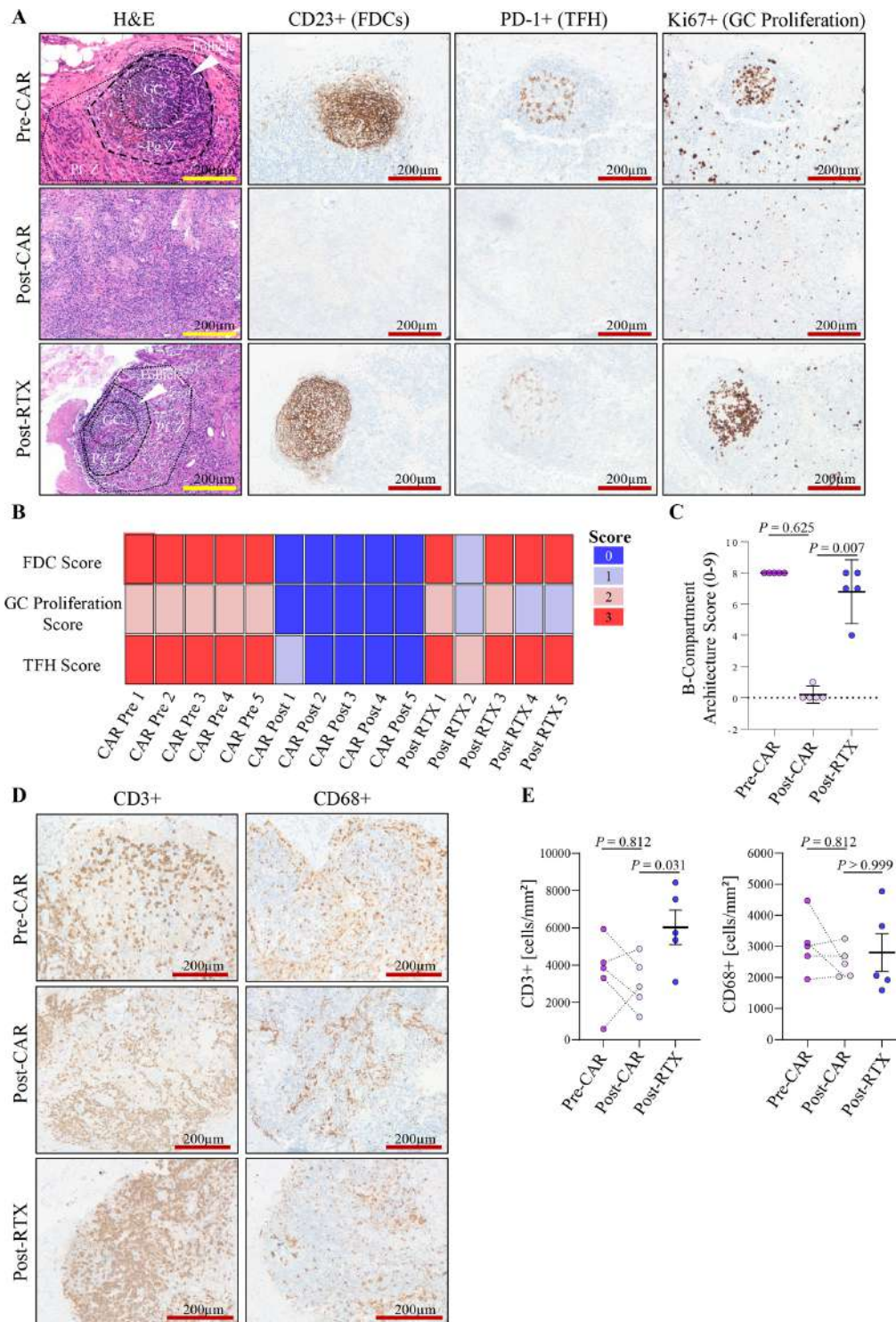
Figure 2 Changes of the B-cell maturation compartment in the lymph nodes (A) Representative H&E-stained images of lymphoid follicles/germinal centres before (pre-CAR) and after (post-CAR) CD19-CAR-T-cell therapy as well as after RTX therapy (post-RTX), together with representative immunohistochemistry pictures of: CD23^{+} follicular dendritic cells (FDCs), PD-1^{+} T follicular helper cells (TFH) and Ki67^{+} proliferating cells in the germinal centres. (B) Heatmap scoring of FDC score, germinal centre proliferation score (GC proliferation score) and the TFH Score. All pre-CAR patients (n=5) and two post-RTX patients had completely unchanged B-cell maturation zones with intact FDC networks and TFH presence as well as high proliferation rates (>90%) of germinal centre B cells (sum score 8). In the other three post-RTX patients (2, 4, 5) a reduced GC proliferation rate (<90%) but preserved or only slightly altered FDC network and TFH presence were found, while all post-CAR T-cell patients presented with completely vanished FDC networks and TFH presence (except one case with few scattered remaining Tfh cells) as well as missing proliferation zones. (C) FDC, GC proliferation and TFH scores summarised in a combined B-cell compartment architecture score. (D) Representative immunohistochemistry images of CD3^{+} T cells and CD68^{+} macrophages in lymph node biopsies before (pre-CAR) and after CAR T-cell (post-CAR) treatment as well as after RTX (post-RTX) treatment. (E) Quantifications of CD3^{+} T cells and CD68^{+} macrophages before (pre-CAR) and after CAR T-cell (post-CAR) treatment (n=5) as well as after RTX (post-RTX) treatment (n=5). CAR, chimeric antigen receptor; GC, germinal centre; Pf. Z, peri-follicular zone; Pg. Z, peri-germinal Zone; RTX, rituximab.

These data suggest that CD138$^+$ cells detected in the lymph node after CD19-CAR T-cell treatment are at the final differentiation stage into plasma cells. This finding is consistent with the persistence of circulating IgG, which decreases following the treatment, but still remains within the normal range, as previously described.[8 9] Persistence of plasma cells was also detected in the lymph nodes of RTX treated patients, as previously reported[5] and none of these patients had hypogammaglobulinemia. However, their proliferation rate was significantly higher than the one after CD19-CAR T-cell treatment.

A comprehensive characterisation of the plasma cell compartment would have required analysis of bone marrow biopsies, which have not been obtained in the present patient cohort. Some data are, however, available from relapsed/refractory large B-cell lymphoma, which was treated with CD19-CAR T-cell therapy.[42] Here, bone marrow biopsies were taken at 58.5 days post therapy, which corresponds to the time we have taken biopsies (60.8 days). Single-cell RNA-sequencing revealed that memory and naive B cells were diminished in the bone marrow, while plasma cells, were not affected.[42] As for the plasma cells, our findings demonstrate that the numbers of other immune cells such as T cells and macrophages were not affected by CD19-CAR T-cell therapy. These findings point against a major role of lymphodepleting therapy, which affects B-lymphocyte and T-lymphocyte populations as well as macrophages in the circulation, bone marrow and other tissues without any specificity or predilection for certain cell populations.[43–45] In this study, we demonstrate that T cells as well as other immune cells such as macrophages are not affected in pre-CAR and post-CAR biopsies and that circulating T cells are not depleted at the time of the biopsy. The persistence of other immune cells in the tissue also suggests that lymphodepletion is unlikely to be responsible for the abrogation of FDCs and TFH, whose disappearance is more reasonably related to the lack of survival signals from B cells.

In summary, this study shows that CD19-CAR T-cell therapy completely depletes B cells in the tissues of patients with AIDs and alters the follicular structure of the lymph nodes. Deep tissue depletion of B cells after CD19-CAR T-cell therapy may likely be based on the fact that (1) antigen binding and effector function are integrated into one and the same cell, (2) CD19-CAR T cells migrate to any tissue of the body and (3) they have the potential to serially kill B cells.[46 47] In addition, lymphodepleting therapy, which is administered in conjunction with CD19-CAR T cells, may add to the depth of B-cell depletion in the tissues. These data highlight the importance of tissue analysis after B-cell depleting therapy in order to quantify the depth of treatment effect.

Author affiliations
[1]Department of Medicine 3—Rheumatology and Immunology, Friedrich-Alexander-Universität (FAU) Erlangen-Nürnberg and Uniklinikum Erlangen, Erlangen, Germany
[2]Deutsches Zentrum Immuntherapie (DZI), Friedrich-Alexander-Universität (FAU) Erlangen-Nürnberg and Uniklinikum Erlangen, Erlangen, Germany, Erlangen, Germany
[3]Division of Rheumatology—Fondazione Policlinico Universitario A. Gemelli, IRCCS—Università Cattolica del Sacro Cuore, Roma, Lazio, Italy
[4]Institute of Pathology and Comprehensive Cancer Center EMN, Friedrich-Alexander-Universität (FAU) Erlangen-Nürnberg and Uniklinikum Erlangen, Erlangen, Germany
[5]Department of Nephropathology, Institute of Pathology, Friedrich-Alexander-Universität (FAU) Erlangen-Nürnberg and Uniklinikum Erlangen, Erlangen, Germany
[6]Department of Medicine 5—Hematology and Oncology, Friedrich-Alexander-Universität Erlangen-Nürnberg (FAU) and Uniklinikum Erlangen, Erlangen, Bayern, Germany

Correction notice This article has been corrected since it published Online First. Figure 1 part E has been corrected.

Competing interests GS has received speaker honoraria from BMS, Cabaletta, Janssen, Kyverna, Miltenyi and Novartis. AM has received speaker honoraria and consulting fees from BMS/Celgene, Kite/Gilead, Novartis, BioNTech, Miltenyi Biomedicine, Century Therapeutics. MADA has received grants or contracts from Amgen, Abbvie, UCB, Pfizer, J&J and Galapagos and speaker honoraria and consulting fees from Abbvie, Amgen, Novartis, BMS, UCB, J&J, Biogen, MSD, Lilly and Galapagos. FM has received speaker honoraria and consulting fees from AstraZeneca, Kite/Gilead, Novartis, Sobi, BMS, Miltenyi, Janssen, BNT.

Patient and public involvement Patients and/or the public were not involved in the design, or conduct, or reporting, or dissemination plans of this research.

Patient consent for publication Not applicable.

Ethics approval This study involves human participants. All procedures were performed in accordance with the Good Clinical Practice guidelines of the International Council for Harmonization and covered by licence 334_18 B of the institutional review board. Self-reported and biological sexes were identical in all patients. All participants gave written informed consent according to CARE guidelines and in compliance with the Declaration of Helsinki principles. No commercial sponsor was involved. Participants gave informed consent to participate in the study before taking part.

Provenance and peer review Not commissioned; externally peer reviewed.

Data availability statement All data relevant to the study are included in the article or uploaded as online supplemental information.

Supplemental material This content has been supplied by the author(s). It has not been vetted by BMJ Publishing Group Limited (BMJ) and may not have been peer-reviewed. Any opinions or recommendations discussed are solely those of the author(s) and are not endorsed by BMJ. BMJ disclaims all liability and responsibility arising from any reliance placed on the content. Where the content includes any translated material, BMJ does not warrant the accuracy and reliability of the translations (including but not limited to local regulations, clinical guidelines, terminology, drug names and drug dosages), and is not responsible for any error and/or omissions arising from translation and adaptation or otherwise.

ORCID iDs
Carlo Tur http://orcid.org/0009-0003-6241-6116
Simon Rauber http://orcid.org/0000-0001-8306-9334
Christina Bergmann http://orcid.org/0000-0001-5257-9171
Ricardo Grieshaber-Bouyer http://orcid.org/0000-0002-2873-5135
Andreas Ramming http://orcid.org/0000-0002-7003-501X
Maria-Antonietta D'Agostino http://orcid.org/0000-0002-5347-0060
Fabian Müller http://orcid.org/0000-0001-5487-5839

Aline Bozec http://orcid.org/0000-0001-8174-2118
Georg Schett http://orcid.org/0000-0001-8740-9615
Maria Gabriella Raimondo http://orcid.org/0000-0003-2020-6711

REFERENCES

1 Lee DSW, Rojas OL, Gommerman JL. B cell depletion therapies in autoimmune disease: advances and mechanistic insights. *Nat Rev Drug Discov* 2021;20:179–99.

2 Dörner T, Isenberg D, Jayne D, *et al*. International Roundtable on B-cells as Therapeutic Target for Intervention. Current status on B-cell depletion therapy in autoimmune diseases other than rheumatoid arthritis. *Autoimmun Rev* 2009;9.

3 Merrill JT, Neuwelt CM, Wallace DJ, *et al*. Efficacy and safety of rituximab in moderately-to-severely active systemic lupus erythematosus: the randomized, double-blind, phase II/III systemic lupus erythematosus evaluation of rituximab trial. *Arthritis Rheum* 2010;62:222–33.

4 Anolik JH, Barnard J, Owen T, *et al*. Delayed memory B cell recovery in peripheral blood and lymphoid tissue in systemic lupus erythematosus after B cell depletion therapy. *Arthritis Rheum* 2007;56:3044–56.

5 Ramwadhdoebe TH, van Baarsen LGM, Boumans MJH, *et al*. Effect of rituximab treatment on T and B cell subsets in lymph node biopsies of patients with rheumatoid arthritis. *Rheumatol (Oxford)* 2019;58:1075–85.

6 Kamburova EG, Koenen HJPM, Borgman KJE, *et al*. A single dose of rituximab does not deplete B cells in secondary lymphoid organs but alters phenotype and function. *Am J Transplant* 2013;13:1503–11.

7 Schett G, Mackensen A, Mougiakakos D. CAR T-cell therapy in autoimmune diseases. *Lancet* 2023;402:2034–44.

8 Mackensen A, Müller F, Mougiakakos D, *et al*. Anti-CD19 CAR T cell therapy for refractory systemic lupus erythematosus. *N Med* 2022;28:2124–32.

9 Müller F, Taubmann J, Bucci L, *et al*. CD19 CAR T-Cell Therapy in Autoimmune Disease - A Case Series with Follow-up. *N Engl J Med* 2024;390:687–700.

10 Pecher A-C, Hensen L, Klein R, *et al*. CD19-Targeting CAR T Cells for Myositis and Interstitial Lung Disease Associated With Antisynthetase Syndrome. *JAMA* 2023;329:2154–62.

11 Wang W, He S, Zhang W, *et al*. BCMA-CD19 compound CAR T cells for systemic lupus erythematosus: a phase 1 open-label clinical trial. *Ann Rheum Dis* 2024.

12 Nicolai R, Merli P, Moran Alvarez P, *et al*. Autologous CD19-Targeting CAR T Cells in a Patient With Refractory Juvenile Dermatomyositis. *Arthritis Rheumatol* 2024.

13 Haghikia A, Hegelmaier T, Wolleschak D, *et al*. Anti-CD19 CAR T cells for refractory myasthenia gravis. *Lancet Neurol* 2023;22:1104–5.

14 Kansal R, Richardson N, Neeli I, *et al*. Sustained B cell depletion by CD19-targeted CAR T cells is a highly effective treatment for murine lupus. *Sci Transl Med* 2019;11:eaav1648.

15 Bankhead P, Loughrey MB, Fernández JA, *et al*. QuPath: Open source software for digital pathology image analysis. *Sci Rep* 2017;7:16878.

16 van Baarsen LGM, de Hair MJH, Ramwadhdoebe TH, *et al*. The cellular composition of lymph nodes in the earliest phase of inflammatory arthritis. *Ann Rheum Dis* 2013;72:1420–4.

17 Fiechter RH, Bolt JW, van de Sande MGH, *et al*. Ultrasound-guided lymph node biopsy sampling to study the immunopathogenesis of rheumatoid arthritis: a well-tolerated valuable research tool. *Arthritis Res Ther* 2022;24:36.

18 Leandro MJ, Cambridge G, Edwards JC, *et al*. B-cell depletion in the treatment of patients with systemic lupus erythematosus: a longitudinal analysis of 24 patients. *Rheumatol (Oxford)* 2005;44:1542–5.

19 Leandro MJ, Cambridge G, Ehrenstein MR, *et al*. Reconstitution of peripheral blood B cells after depletion with rituximab in patients with rheumatoid arthritis. *Arthritis Rheum* 2006;54:613–20.

20 Breedveld F, Agarwal S, Yin M, *et al*. Rituximab pharmacokinetics in patients with rheumatoid arthritis: B-cell levels do not correlate with clinical response. *J Clin Pharmacol* 2007;47:1119–28.

21 Audia S, Samson M, Guy J, *et al*. Immunologic effects of rituximab on the human spleen in immune thrombocytopenia. *Blood* 2011;118:4394–400.

22 Thurlings RM, Vos K, Wijbrandts CA, *et al*. Synovial tissue response to rituximab: mechanism of action and identification of biomarkers of response. *Ann Rheum Dis* 2008;67:917–25.

23 Rehnberg M, Amu S, Tarkowski A, *et al*. Short- and long-term effects of anti-CD20 treatment on B cell ontogeny in bone marrow of patients with rheumatoid arthritis. *Arthritis Res Ther* 2009;11:R123.

24 Looney CM, Schroeder A, Tavares E, *et al*. Obinutuzumab Effectively Depletes Key B-cell Subsets in Blood and Tissue in End-stage Renal Disease Patients. *Transplant Direct* 2023;9:e1436.

25 Kantarjian H, Stein A, Gökbuget N, *et al*. Blinatumomab versus Chemotherapy for Advanced Acute Lymphoblastic Leukemia. *N Engl J Med* 2017;376:836–47.

26 Bargou R, Leo E, Zugmaier G, *et al*. Tumor regression in cancer patients by very low doses of a T cell-engaging antibody. *Science* 2008;321:974–7.

27 Bucci L, Hagen M, Rothe T, *et al*. Bispecific T cell engager therapy for refractory rheumatoid arthritis. *Nat Med* 2024;30:1593–601.

28 He H, Chen S, Yu Y, *et al*. Comprehensive single-cell analysis deciphered microenvironmental dynamics and immune regulator olfactomedin 4 in pathogenesis of gallbladder cancer. *Gut* 2024.:gutjnl-2023-331773.

29 Schenk M, Mueller C. The mucosal immune system at the gastrointestinal barrier. *Best Pract Res Clin Gastroenterol* 2008;22:391–409.

30 Arazi A, Rao DA, Berthier CC, *et al*. The immune cell landscape in kidneys of patients with lupus nephritis. *Nat Immunol* 2019;20:902–14.

31 Schriever F, Freedman AS, Freeman G, *et al*. Isolated human follicular dendritic cells display a unique antigenic phenotype. *J Exp Med* 1989;169:2043–58.

32 Abd El-Aleem SA, Saber EA, Aziz NM, *et al*. Follicular dendritic cells. *J Cell Physiol* 2022;237:2019–33.

33 Murphy M, Walter BN, Pike-Nobile L, *et al*. Expression of the lymphotoxin beta receptor on follicular stromal cells in human lymphoid tissues. *Cell Death Differ* 1998;5:497–505.

34 Cupedo T, Lund FE, Ngo VN, *et al*. Initiation of cellular organization in lymph nodes is regulated by non-B cell-derived signals and is not dependent on CXC chemokine ligand 13. *J Immunol* 2004;173:4889–96.

35 Tumanov A, Kuprash D, Lagarkova M, *et al*. Distinct role of surface lymphotoxin expressed by B cells in the organization of secondary lymphoid tissues. *Immunity* 2002;17:239–50.

36 Fütterer A, Mink K, Luz A, *et al*. The lymphotoxin beta receptor controls organogenesis and affinity maturation in peripheral lymphoid tissues. *Immunity* 1998;9:59–70.

37 Cerny A, Zinkernagel RM, Groscurth P. Development of follicular dendritic cells in lymph nodes of B-cell-depleted mice. *Cell Tissue Res* 1988;254:449–54.

38 Endres R, Alimzhanov MB, Plitz T, *et al*. Mature follicular dendritic cell networks depend on expression of lymphotoxin beta receptor by radioresistant stromal cells and of lymphotoxin beta and tumor necrosis factor by B cells. *J Exp Med* 1999;189:159–68.

39 Baumjohann D, Preite S, Reboldi A, *et al*. Persistent antigen and germinal center B cells sustain T follicular helper cell responses and phenotype. *Immunity* 2013;38:596–605.

40 Yusuf I, Stern J, McCaughtry TM, *et al*. Germinal center B cell depletion diminishes CD4+ follicular T helper cells in autoimmune mice. *PLoS ONE* 2014;9:e102791.

41 Audia S, Rossato M, Trad M, *et al*. B cell depleting therapy regulates splenic and circulating T follicular helper cells in immune thrombocytopenia. *J Autoimmun* 2017;77:89–95.

42 Strati P, Li X, Deng Q, *et al*. Prolonged cytopenia following CD19 CAR Tcell therapy is linked with bone marrow infiltration of clonally expanded IFNγ-expressing CD8 Tcells. *Cell Rep Med* 2023;4:101158.

43 Hurd ER, Giuliano VJ. The effect of cyclophosphamide on B and T lymphocytes in patients with connective tissue diseases. *Arthritis Rheum* 1975;18:67–75.

44 Winkelstein A. Mechanisms of immunosuppression: effects of cyclophosphamide on cellular immunity. *Blood* 1973;41:273–84.

45 Gassner FJ, Weiss L, Geisberger R, *et al*. Fludarabine modulates composition and function of the T cell pool in patients with chronic lymphocytic leukaemia. *Cancer Immunol Immunother* 2011;60:75–85.

46 Porter DL, Levine BL, Kalos M, *et al*. Chimeric antigen receptor-modified T cells in chronic lymphoid leukemia. *N Engl J Med* 2011;365:725–33.

47 Davenport AJ, Jenkins MR, Cross RS, *et al*. CAR-T Cells Inflict Sequential Killing of Multiple Tumor Target Cells. *Cancer Immunol Res* 2015;3:483–94.

48 Carter LM, Gordon C, Yee C-S, *et al*. Easy-BILAG: a new tool for simplified recording of SLE disease activity using BILAG-2004 index. *Rheumatol (Oxford)* 2022;61:4006–15.